

A novel method for solving structural problems: Elastoplastic analysis of a pressurized thick heterogeneous sphere

Abbas Heydari*

Department of Civil Engineering, Technical and Vocational University (TVU), Tehran, Iran

(Received March 16, 2023, Revised January 31, 2024, Accepted February 19, 2024)

Abstract. If the governing differential equation arising from engineering problems is treated as an analytic, continuous and derivable function, it can be expanded by one point as a series of finite numbers. For the function to be zero for each value of its domain, the coefficients of each term of the same power must be zero. This results in a recursive relationship which, after applying the natural conditions or the boundary conditions, makes it possible to obtain the values of the derivatives of the function with acceptable accuracy. The elastoplastic analysis of an inhomogeneous thick sphere of metallic materials with linear variation of the modulus of elasticity, yield stress and Poisson's ratio as a function of radius subjected to internal pressure is presented. The Beltrami-Michell equation is established by combining equilibrium, compatibility and constitutive equations. Assuming axisymmetric conditions, the spherical coordinate parameters can be used as principal stress axes. Since there is no analytical solution, the natural boundary conditions are applied and the governing equations are solved using a proposed new method. The maximum effective stress of the von Mises yield criterion occurs at the inner surface; therefore, the negative sign of the linear yield stress gradation parameter should be considered to calculate the optimal yield pressure. The numerical examples are performed and the plots of the numerical results are presented. The validation of the numerical results is observed by modeling the elastoplastic heterogeneous thick sphere as a pressurized multilayer composite reservoir in Abaqus software. The subroutine USDFLD was additionally written to model the continuous gradation of the material.

Keywords: elastoplastic analysis; internal pressure; mechanical properties variation; novel numerical method; thick sphere

1. Introduction

Compared to conventional composite laminates, they offer several advantages, such as resistance to very high temperature gradients, lower stress concentrations, higher corrosion resistance, higher toughness and higher fracture strength. Therefore, many researchers have focused their attention on studying the mechanical behavior of structures made of functionally graded materials (FGMs). Elasto-plastic analysis of thick-walled functionally graded tanks subjected to internal pressure has been elaborated (Heydari 2009). The residual stress distribution in autofrettage homogeneous spherical pressure vessels subjected to different autofrettage pressures is evaluated (Maleki *et al.* 2010). The Armstrong-Frederick kinematic hardening model

*Corresponding author, Ph.D., E-mail: a_heydari@tabrizu.ac.ir

is adopted and Voce's hardening law is included for isotropic hardening behavior (Leu *et al.* 2014). An analytical solution of thick-walled piezoelectric functionally graded (FG) cylinder for non-axisymmetric thermo-mechanical loads and uniform electric field is carried out (Atrian *et al.* 2015). The two-dimensional analytical solution of a piezothermoelastic FG hollow sphere with integrated piezoelectric layers as a sensor and actuator for non-axisymmetric loads is calculated by using the system of Euler differential equations and Legendre polynomials (Barati and Jabbari 2015). Spreading of plastic zones in functionally graded spherical tanks subjected to internal pressure and temperature gradient combinations is investigated (Heydari 2015). The active control of FG hollow sphere's displacement and stress is performed by applying a feedback gain control algorithm. An analytical size-dependent model is proposed based on electro-elastic surface/interface model to investigate the dynamic electromechanical response of a multilayer piezoelectric nano-cylinder subjected to electro-elastic waves by considering interface energy effect on the stress and electric field (Fang *et al.* 2015). The power law function is used to analyze snap-through buckling behavior of shallow clamped FG spherical shell with surface-bonded piezoelectric actuators subjected to the thermo-electro-mechanical loading (Sabzikar and Eslami 2014). The Variational Asymptotic Method (VAM) splits a 3-D elasticity problem into a 2-D linear cross-sectional problem and a one-dimensional beam problem. A complete agreement between results of commercially available 3-D FEM solver Abaqus and asymptotically exact analytical solutions for FG cylinder based on VAM is observed (Sachdeva and Padhee 2018). Many elastoplastic analyses are performed (Ushio *et al.* 2019, Masoodi 2019, Polatov *et al.* 2020). Elastoplastic analysis of thick-walled vessels with isotropic strain hardening behavior using nonlinear compatibility relation is done (Heydari 2018). An exact solution of 3-D elasticity for sound transmission loss through FG cylinder in the presence of subsonic external flow by modeling through-thickness gradation of materials based on power law function is obtained (Daneshjou *et al.* 2017). The nonlinear analysis of functionally graded spherical pressure vessels composed of metal/ceramic mixture for both high strength and high thermal resistance is discussed (Yildirim *et al.* 2022). The use of recursive algorithm to formulate the analytical solution of thermo-mechanical stresses of multi-layered hollow spherical pressure vessel is demonstrated (Sim *et al.* 2021). The plastic limit pressure of spherical vessels of nonlinear combined isotropic/kinematic hardening materials is investigated.

The numerical and semi-analytical methods are employed to solve homogeneous or heterogeneous hollow cylinder problems. Elastoplastic analysis of cylindrical vessel with arbitrary material gradation subjected to thermo-mechanical loading via DTM is conducted (Heydari 2019). The mechanical stress reduction in a pressurized 2D-FGM thick hollow cylinder with finite length is studied (Najibi 2017). The meshless local Petrov-Galerkin method is employed to investigate dynamic response of FG viscoelastic hollow cylinder subjected to thermo-mechanical loads (Akbari *et al.* 2018). The meshless local Petrov-Galerkin method based on total Lagrangian approach is applied for geometrically nonlinear analysis of a FG thick-walled hollow cylinder with Rayleigh damping subjected to axisymmetric mechanical shock loading (Ghadiri Rad *et al.* 2015). The perturbation method is applied to describe dispersion curves in the neighborhood of radial resonances for an isotropic hollow cylinder in the presence of an inhomogeneous prestress field (Vatul'yan and Yurov 2016). The differential quadrature method (DQM) is applied to study the Electro-elasto-dynamic analysis of FG cylindrical shell with piezoelectric rings (Saviz, 2017).

Most of engineering problems must be solved numerically (Oh *et al.* 2023, Babaei *et al.* 2022, Zaid and Sadique 2020, Fenjan *et al.* 2020, Heydari 2017). Nowadays, the new numerical methods are proposed and their progress is still increasing with day to day. In this study, a new numerical

method is introduced for solving structural problems and outcomes are verified by FEM results. The governing differential equations of various engineering problems such as elastoplastic analysis of thick heterogeneous reservoir can be solved by the proposed method. Fast convergence and compatibility with various conditions are advantages of proposed method however, the method may have convergence problem in nonlinear ODEs. The stress and strain fields of a spherical reservoir with through-the-thickness variation of mechanical properties subjected to internal pressure is obtained using proposed method to present the efficiency and accuracy of the new method. The elastoplastic analysis of the inhomogeneous thick sphere of metallic materials with linear variation of elastic modulus, yield stress and Poisson's ratio in terms of radius subjected to internal pressure is presented. The Beltrami-Michell equation is established by combining equilibrium, compatibility and constitutive equations. By assuming axisymmetric conditions, the spherical coordinate parameters can be used as principal stress axes. The natural boundary conditions are applied and the governing equations are solved using the proposed method, since there is no analytical solution.

2. Governing equations

The basic equations are simplified because of the axisymmetric conditions. The equilibrium and compatibility equations are simplified as follows:

$$\frac{d}{dr} \sigma_r(r) + \frac{2(\sigma_r(r) - \sigma_\theta(r))}{r} = 0 \quad (1)$$

$$\frac{d}{dr} \epsilon_\theta(r) + \frac{\epsilon_\theta(r) - \epsilon_r(r)}{r} = 0 \quad (2)$$

Hooke's constitutive relation is used because of the linear material behavior in the elastic zone.

$$\epsilon_r(r) = \frac{\sigma_r(r) - 2\nu\sigma_\theta(r)}{E(r)} \quad (3)$$

$$\epsilon_\theta(r) = \frac{(1 - \nu)\sigma_\theta(r) - \nu\sigma_r(r)}{E(r)} \quad (4)$$

The governing equation in terms of radial stress is calculated by considering Eq. (1) to Eq. (4).

$$\phi_1(r) \frac{d^2}{dr^2} \sigma_r(r) + \phi_2(r) \frac{d}{dr} \sigma_r(r) + \phi_3(r) \sigma_r(r) = 0 \quad (5)$$

The coefficients ϕ_1 to ϕ_3 are

$$\phi_1(r) = -rE(r)(\nu(r) - 1) \quad (6)$$

$$\phi_2(r) = r(\nu(r) - 1) \frac{d}{dr} E(r) - E(r) \left(r \frac{d}{dr} \nu(r) + 4\nu(r) - 4 \right) \quad (7)$$

$$\phi_3(r) = -4 \left(\left(\frac{1}{2} - \nu(r) \right) \frac{d}{dr} E(r) + E(r) \frac{d}{dr} \nu(r) \right) \quad (8)$$

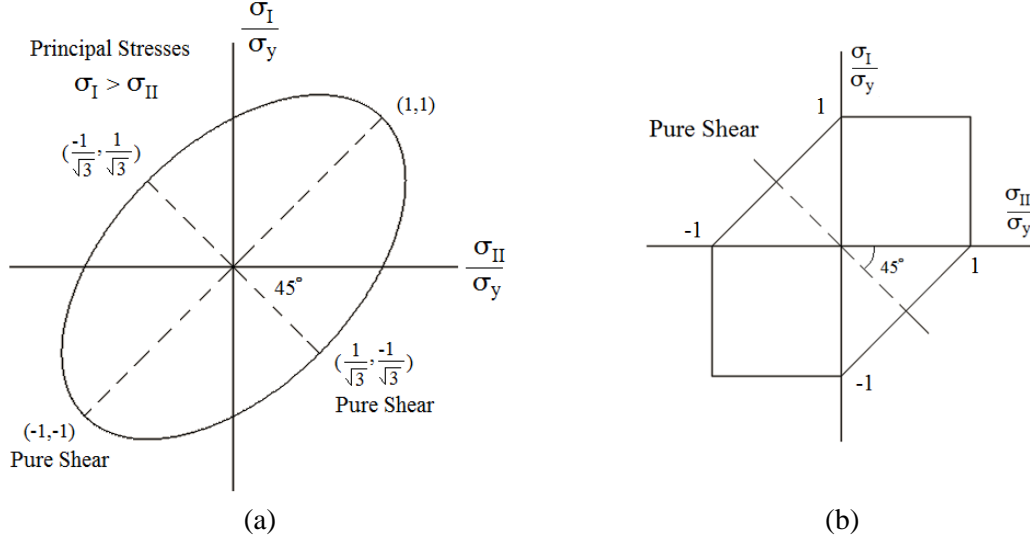


Fig. 1 Yield criteria (a): von Mises and (b): Tresca in the dimensionless coordinate system

The functions of the mechanical properties, i.e. Young's modulus, yield stress and Poisson's ratio are linear functions in terms of the radius in the spherical coordinate system.

$$E(r) = E_o + E_s r \quad (9)$$

$$\sigma_y(r) = \sigma_{y0} + \sigma_{ys} r \quad (10)$$

$$\nu(r) = \nu_o + \nu_s r \quad (11)$$

where the parameters E_o and ν_o with index zero denote the value of the mechanical property at the center. The parameters E_s and ν_s refer to the linear material gradation. The modulus of elasticity and Poisson's ratio are inserted into the coefficients of the second-order differential equation. These coefficients are rewritten as follows:

$$\phi_1(r) = -(E_o r + E_s r^2)(\nu_o + \nu_s r - 1) \quad (12)$$

$$\phi_2(r) = (\nu_o r + \nu_s r^2 - r)E_s - (E_o + E_s r)(5\nu_s r - 4(1 - \nu_o)) \quad (13)$$

$$\phi_3(r) = (4\nu_o - 2)E_s - 4E_o \nu_s \quad (14)$$

The von Mises yield criterion is an ellipse with no singularity in the principal axis coordinate. The axisymmetric condition means that the first and second principal axes are radial and tangential axes, respectively, in the spherical coordinate system ($\sigma_I = \sigma_r, \sigma_{II} = \sigma_{III} = \sigma_\theta = \sigma_\phi$).

The von Mises and Tresca yield criteria can be expressed by the principal axes.

$$\frac{1}{6}(\sigma_I - \sigma_{II})^2 + \frac{1}{6}(\sigma_I - \sigma_{III})^2 + \frac{1}{6}(\sigma_{II} - \sigma_{III})^2 = \frac{1}{3}\sigma_y^2 \quad (15)$$

$$\frac{1}{2}\max(|\sigma_I - \sigma_{II}|, |\sigma_I - \sigma_{III}|, |\sigma_{II} - \sigma_{III}|) = \frac{1}{2}\sigma_y \quad (16)$$

After considering axisymmetric conditions, final results of the both yield criteria are similar.

$$|\sigma_r - \sigma_\theta| = \sigma_y \quad (17)$$

Combining Eq. (1) and Eq. (17), we obtain

$$\frac{d}{dr} \sigma_r(r) - \frac{2}{r} (\sigma_{y0} + \sigma_{ys} r) = 0 \quad (18)$$

3. Novel numerical method

The relevant differential equation must be solved using a numerical method. In mathematics, a collocation method is a method for numerically solving ordinary differential equations, partial differential equations and integral equations. The idea is to choose a finite-dimensional space of possible solutions (usually polynomials up to a certain degree) and a number of points in this space (called collocation points) and choose the solution that satisfies the given equation at the collocation points. The same idea is used, but the values of the derivatives of the function with acceptable accuracy are considered without calculating the coefficients of a candidate polynomial. The equation (5) is rewritten as follows:

$$f(r) = \phi_1(r) \frac{d^2}{dr^2} \sigma_r(r) + \phi_2(r) \frac{d}{dr} \sigma_r(r) + \phi_3(r) \sigma_r(r) = 0 \quad (19)$$

Maclaurin series expansion of the function f in Eq. (19) is

$$f(r) = \sum_{n=0}^m F_n r^n = \sum_{n=0}^m \frac{r^n}{n!} \left[\frac{d^n}{dr^n} f(r) \right]_{r=0} \quad m \in \mathbb{N} \quad (20)$$

The function f for any value of its domain ($a \leq r \leq b$) must vanish, where a and b are inner and outer radius of sphere.

$$f(r) = \left(\sum_{k=0}^n \frac{n!}{k! (n-k)!} (\tilde{\phi}_1 + \tilde{\phi}_2 + \tilde{\phi}_3) \Big|_{r=0} \right) r^n = 0 \quad (21)$$

Since all terms of the approximation of the function f in Eq. (19) with similar powers of r must vanish, one can write

$$\sum_{k=0}^n \frac{n!}{k! (n-k)!} (\tilde{\phi}_1 + \tilde{\phi}_2 + \tilde{\phi}_3) \Big|_{r=0} \quad (22)$$

in which,

$$\varphi_i(n, k, r) = \sum_{k=0}^n \frac{n!}{k! (n-k)!} \tilde{\phi}_i \quad i \in \{1, 2, 3\} \quad (23)$$

The parameters φ_1 to φ_3 are

$$\varphi_1(n, k, r) = \sum_{k=0}^n \frac{n!}{k! (n-k)!} \frac{d^k}{dr^k} \phi_1(r) \frac{d^{n-k+2}}{dr^{n-k+2}} \sigma_r(r) \quad (24)$$

$$\varphi_2(n, k, r) = \sum_{k=0}^n \frac{n!}{k!(n-k)!} \frac{d^k}{dr^k} \phi_2(r) \frac{d^{n-k+1}}{dr^{n-k+1}} \sigma_r(r) \quad (25)$$

$$\varphi_3(n, k, r) = \sum_{k=0}^n \frac{n!}{k!(n-k)!} \frac{d^k}{dr^k} \phi_3(r) \frac{d^{n-k}}{dr^{n-k}} \sigma_r(r) \quad (26)$$

After substituting Eqs. (12) to (14) in Eqs. (24) to (26), the parametrs φ_1 to φ_3 are simplified.

$$\varphi_1|_{r=0} = (nE_o(1 - \nu_o)\varsigma_{n+1} + n(n-1)(E_s(1 - \nu_o) - E_o\nu_s)\varsigma_n) \quad (27)$$

$$\varphi_2|_{r=0} = (4E_o(1 - \nu_o)\varsigma_{n+1} + n(3E_s(1 - \nu_o) - 5E_o\nu_s)\varsigma_n - 4n(n-1)\nu_s E_s \varsigma_{n-1}) \quad (28)$$

$$\varphi_3|_{r=0} = ((4\nu_o - 2)E_s - 4E_o\nu_s)\varsigma_n \quad (29)$$

where the ς_n is the differential transform of the n^{th} derivative of function $\sigma_r(r)$ is defined as follows:

$$\varsigma_n = \frac{1}{n!} \left[\frac{d^n}{dr^n} \sigma_r(r) \right]_{r=0} \quad (30)$$

Substituting Eqs. (27) to (29) in Eq. (22), the recursive equation is extracted.

$$\varsigma_{n+1} = \frac{\eta_3}{\eta_1} \varsigma_{n-1} - \frac{\eta_2}{\eta_1} \varsigma_n \quad n \in \mathbb{N} \quad (31)$$

Where

$$\eta_1 = (1 - \nu_o)E_o(n + 4) \quad (32)$$

$$\eta_2 = ((1 - \nu_o)(n^2 + 2n) - 2(1 - 2\nu_o))E_s - E_o\nu_s(n + 2)^2 \quad (33)$$

$$\eta_3 = 4\nu_s E_s n(n - 1) \quad (34)$$

The boundary conditions are $\sigma_r(a) = -P$ and $\sigma_r(b) = 0$, where P is internal pressure. It holds

$$\varsigma_0 = \left(\frac{a}{b-a} \right) \left(\sum_{k=2}^n \varsigma_k (b^k - a^k) \right) - \sum_{k=2}^n \varsigma_k a^k - \frac{Pb}{b-a} \quad (35)$$

$$\varsigma_1 = - \left(\frac{b}{b-a} \right) \sum_{k=2}^n \varsigma_k b^{k-1} + \frac{1}{b-a} \left(\sum_{k=2}^n \varsigma_k a^k + P \right) \quad (36)$$

The circumferential stress in elastic zone can be obtained as follows:

$$\sigma_\theta(r) = \sum_{k=0}^n \varsigma_k r^k + \frac{1}{2} \sum_{k=1}^n \varsigma_k k r^k \quad (37)$$

The elastic strain field is calculated as follows:

Table 1 Numerical values of geometry, loading and mechanical properties

a (cm)	b (cm)	P_y (Kg/cm ²)	E_o (kg/cm ²)	E_s (kg/cm ³)	ν_o	ν_s (cm ⁻¹)	σ_{y_o} (kg/cm ²)	σ_{y_s} (kg/cm ³)
40	50	890	1.5×10^6	2×10^4	0.2	0.003	1400	30

$$\epsilon_r(r) = \frac{(1 - 2\nu) \sum_{k=0}^n \zeta_k r^k - \nu \sum_{k=1}^n \zeta_k k r^k}{E_o + E_s r} \quad (38)$$

$$\epsilon_\theta(r) = \frac{(1 - 2\nu) \sum_{k=0}^n \zeta_k r^k + (1 - \nu) \sum_{k=1}^n \zeta_k k r^k / 2}{E_o + E_s r} \quad (39)$$

In contrast to the circumferential displacement, the radial displacement is nonzero.

$$u_r(r) = \frac{(1 - 2\nu) \sum_{k=0}^n \zeta_k r^{k+1} + (1 - \nu) \sum_{k=1}^n \zeta_k k r^{k+1} / 2}{E_o + E_s r} \quad (40)$$

The von Mises yield criterion (also known as the maximum deformation energy criterion) states that yielding of a ductile material begins when the second deviatoric stress invariant reaches a critical value. It is part of the plasticity theory that is most applicable to ductile materials, such as some metals. The effective stress is calculated as follows:

$$\sigma_{\text{eff}} = \frac{1}{2} \sigma_\theta - \frac{1}{2} \sigma_r \quad (41)$$

The onset of plastic yielding condition at inner radius is written as follows:

$$\sum_{k=1}^n \zeta_k k a^k = 2\sigma_y \quad (42)$$

The radial stress in the plastic zone is calculated by solving the governing differential equation of the plastic zone. The circumferential stress can be calculated by considering the equilibrium equation.

$$\sigma_r^p(r) = 2\sigma_{y_0} \ln\left(\frac{r}{a}\right) + 2r\sigma_{y_s} - (2a\sigma_{y_s} + P) \quad (43)$$

$$\sigma_\theta^p(r) = 2\sigma_{y_0} \ln\left(\frac{r}{a}\right) + (3r - 2a)\sigma_{y_s} + \sigma_{y_0} - P \quad (44)$$

The capacity of the reservoir with elastic, perfectly plastic behavior is calculated by approaching the radius of elastic and plastic zones' boundary (i.e. c) to the outer radius, b .

$$P_{\text{max}} = 2\sigma_{y_0} \ln\left(\frac{b}{a}\right) + 2\sigma_{y_s}(b - a) \quad (45)$$

4. Results and discussion

The numerical values of the parameters are listed in Table (1) to perform a numerical example. Fig. (2) shows the convergence of numerical results for the case where 30 percent of the

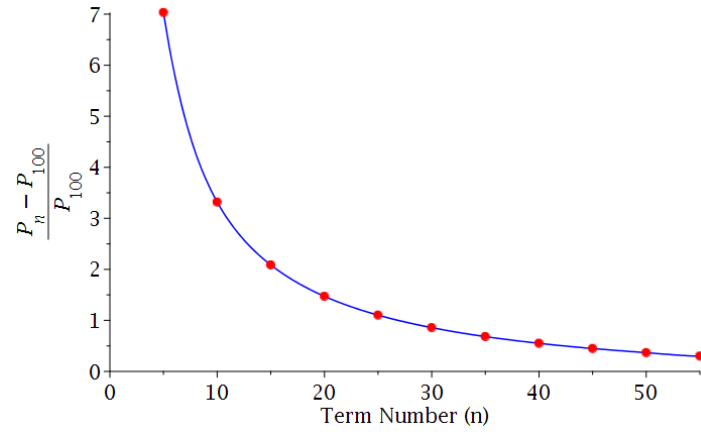


Fig. 2 The convergence of proposed method (R = 30%)

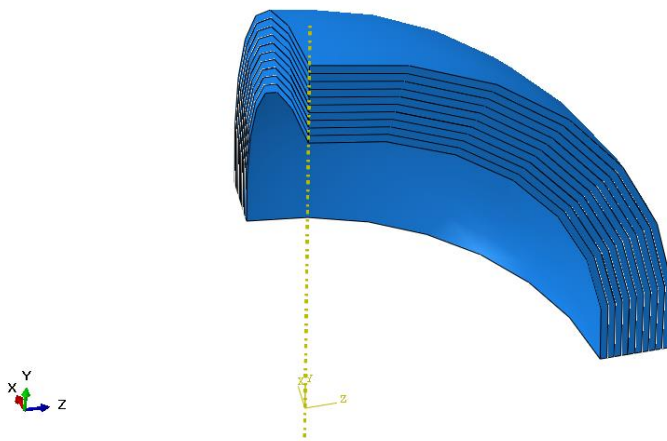


Fig. 3 The equivalent Abaqus model

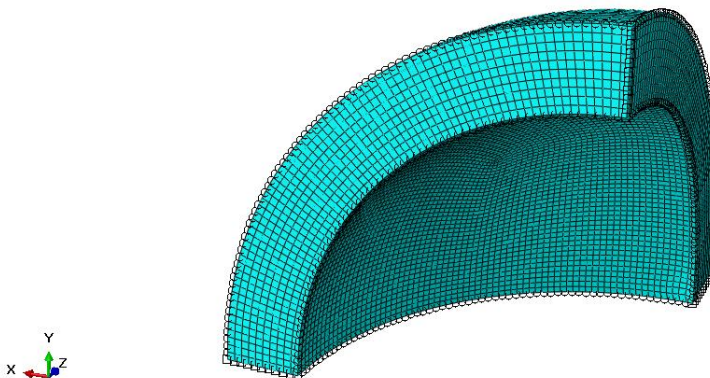


Fig. 4 Model mesh

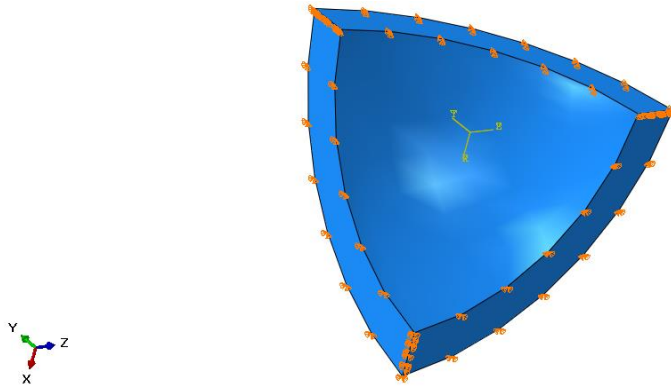


Fig. 5 The boundary conditions compatible with axisymmetric conditions

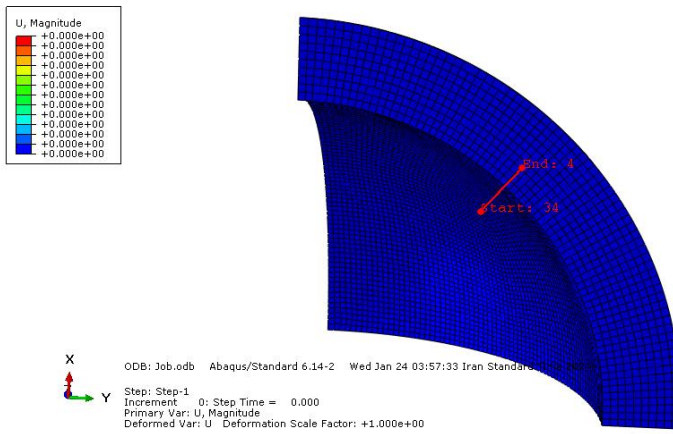


Fig. 6 The defined path in radial direction

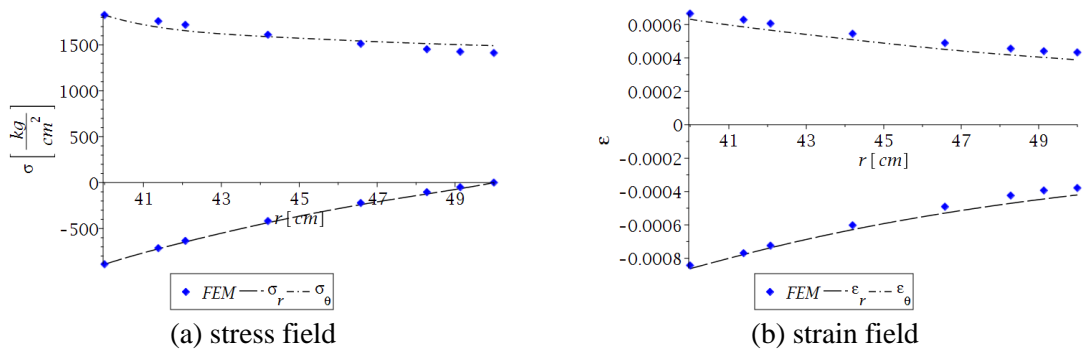


Fig. 7 Comparison between results of proposed method and Abaqus outcomes for onset of yielding

thickness becomes plastic ($R = ((c - a)/(b - a)), P = 1061.2 \text{ kg}$). The equivalent laminated sphere is modeled in Abaqus software. The mechanical and geometrical properties of each layer in Fig. (3) are calculated and presented in Table (2). Since the production of a FG sphere is very expensive, the FEM is used. A good agreement was found between the FEM results and the results

Table 1 Numerical values of geometry, loading and mechanical properties

Layer number (n)	r_i (cm)	r_o (cm)	r_n (cm)	E_n (kg/cm ²)	ν_n	σ_{yn} (kg/cm ²)
1	40	41	40.50	2.310E+06	0.322	2615
2	41	42	41.50	2.330E+06	0.325	2645
3	42	43	42.50	2.350E+06	0.328	2675
4	43	44	43.50	2.370E+06	0.331	2705
5	44	45	44.50	2.390E+06	0.334	2735
6	45	46	45.50	2.410E+06	0.337	2765
7	46	47	46.50	2.430E+06	0.340	2795
8	47	48	47.50	2.450E+06	0.343	2825
9	48	49	48.50	2.470E+06	0.346	2855
10	49	50	49.50	2.490E+06	0.349	2885

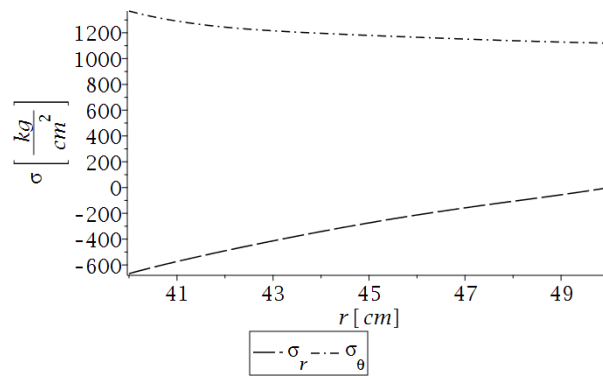


Fig. 8 The stress field in the elastic container

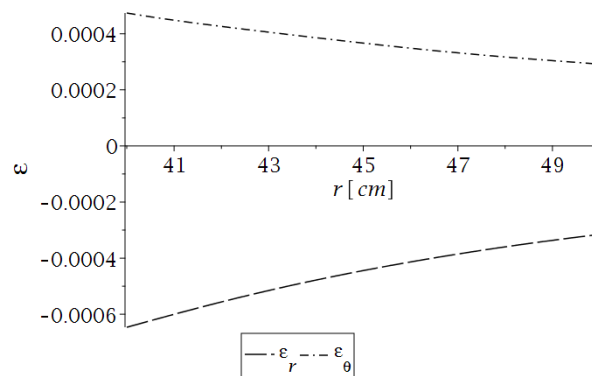


Fig. 9 The strain field in the elastic container

of current research. One-eighth of the original container is modeled based on axisymmetric conditions. According to Fig. (4), elements of type C3D8 with the size of 7.5 mm are used and according to Fig. (5) for preventing of rotation in perpendicular directions the appropriate boundary conditions in spherical coordinate system are applied. To analysis behavior of the graded material, the subroutine USDFLD is additionally written to model the continuous gradation of the

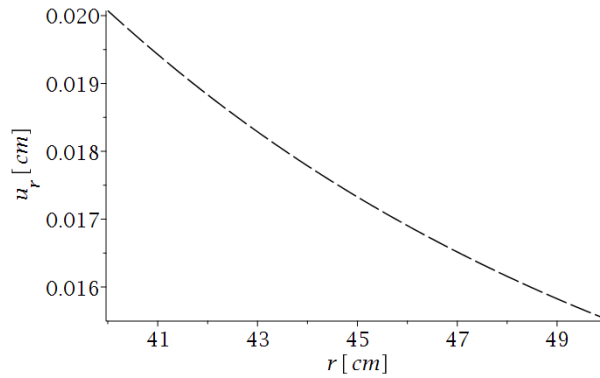


Fig. 10 The radial displacement in the elastic container

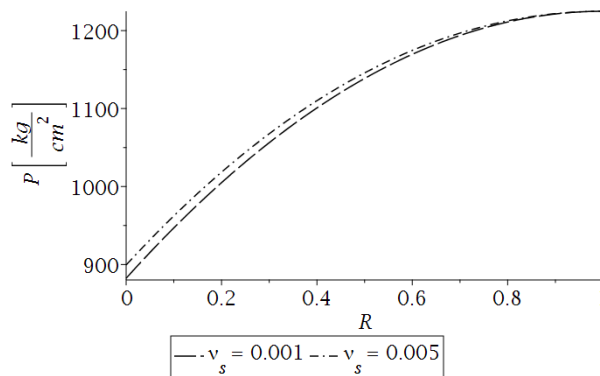


Fig. 11 The effect of gradation of Poisson's ratio on plastic zone propagation

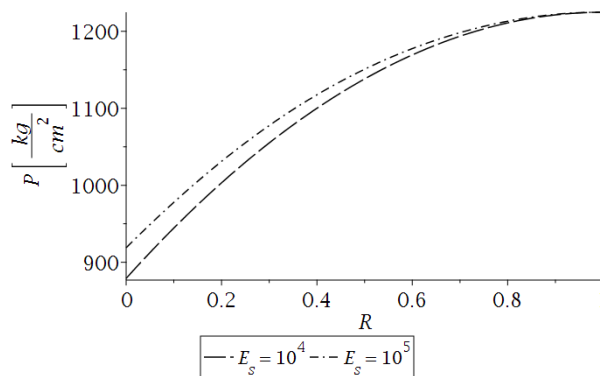


Fig. 12 The effect of gradation of elasticity modulus on plastic zone propagation

material. The proper way to extract the analysis results is shown in Fig. (6). The good agreement between the results of proposed method and the results of FEM can be observed in Fig. (7-a) and (7-b). The other results can be obtained from the stress field. Hooke's law provides the strain field from the stress field and the relative displacement can be calculated directly from the radial strain. Therefore, only the stress field is verified in Fig. (7).

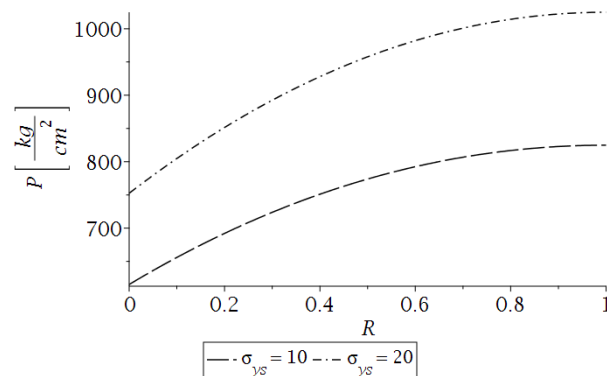


Fig. 13 The effect of yield stress gradation on plastic zone propagation

The elastic stress field is shown in Fig. (8) for $P = 667 \text{ Kg/cm}^2$. Unlike the circumferential stress, the radial stress has a negative sign. In addition, the radial stress on the outer surface has disappeared. The elastic strain field is shown in Fig. (9). Similar to the stress field, the strain in the radial direction has a negative sign and the tangential strain has a positive sign. In contrast to the radial stress, the radial strain at the outer surface is non-zero. The maximum amounts of circumferential stress and strain occur at the inner surface. The maximum absolute amounts of radial stress and strain occur at the inner surface. The radial displacement in the elastic spherical reservoir with linear material variation is shown in Fig. (10). The radial displacement decreases with increasing distance from the inner surface.

The effects of material gradation on the required internal pressure for the propagation of the plastic region are shown in Figs. (11)-(13).

5. Conclusions

A novel and efficient numerical method is proposed to solve the governing differential equation arising from engineering problems. Fast convergence and compatibility with various conditions are the advantages of the proposed method. An elastoplastic, heterogeneous, isotropic, thick-walled sphere is analyzed in the light of the efficiency of the proposed method. The composite sphere model with a limited number of layers is suitable for modeling a heterogeneous thick sphere with a continuous change in mechanical properties subjected to internal pressure. In contrast to the internal pressure, which is necessary for the propagation of the plastic zone, the capacity of the thick-walled sphere with elastic-perfect plastic material behavior is independent of the Poisson's ratio and the variation of the elastic modulus. In addition, the positive change in yield stress increases the internal pressure required to propagate the plastic zone.

References

- Akbari, A., Bagri, A. and Natarajan, S. (2018), "Dynamic response of viscoelastic functionally graded hollow cylinder subjected to thermo-mechanical loads", *Compos. Struct.*, **201**, 414-422.
<https://doi.org/10.1016/j.compstruct.2018.06.044>
- Atrian, A., Jafari Fesharaki, J. and Nourbakhsh, S.H. (2015), "Thermo-electromechanical behavior of

- functionally graded piezoelectric hollow cylinder under non-axisymmetric loads”, *Appl. Math. Mech.*, **36**(7), 939-954. <https://doi.org/10.1007/s10483-015-1959-9>
- Babaei M.i, Atasoy A., Hajirasouliha I., Mollaei S. and Jalilkhani M. (2022), “Numerical solution of beam equation using neural networks and evolutionary optimization tools”, *Adv. Comp. Des.*, **7**(1), 1-17, <https://doi.org/10.12989/acd.2022.7.1.001>
- Barati, A.R. and Jabbari, M. (2015), “Two-dimensional piezothermoelastic analysis of a smart FGM hollow sphere”, *Acta Mech.*, **226**(7), 2195-2224. <https://doi.org/10.1007/s00707-015-1304-8>
- Daneshjou, K., Talebitooti, R. and Tarkashvand, A. (2017), “An exact solution of three-dimensional elasticity for sound transmission loss through FG cylinder in presence of subsonic external flow”, *Int. J. Mech. Sci.*, **120**, 105-119. <https://doi.org/10.1016/j.ijmecsci.2016.10.008>
- Fang, X.Q., Liu, H.W., Feng, W.J. and Liu, J.X. (2015), “Size-dependent effects on electromechanical response of multilayer piezoelectric nano-cylinder under electro-elastic waves”, *Compos. Struct.*, **125**, 23-28. <https://doi.org/10.1016/j.compstruct.2015.01.046>
- Fenjan R.M., Ahmed R.A., Hamad L.B. and Faleh N.M. (2020), “A review of numerical approach for dynamic response of strain gradient metal foam shells under constant velocity moving loads”, *Adv. Comp. Des.*, **5**(4), <https://doi.org/10.12989/acd.2020.5.4.349>
- Ghadiri Rad, M.H., Shahabian, F. and Hosseini, S.M. (2015), “A meshless local Petrov–Galerkin method for nonlinear dynamic analyses of hyper-elastic FG thick hollow cylinder with Rayleigh damping”, *Acta Mech.*, **226**(5), 1497-1513. <https://doi.org/10.1007/s00707-014-1266-2>
- Heydari, A. (2015), “Spreading of Plastic Zones in Functionally Graded Spherical Tanks Subjected to Internal Pressure and Temperature Gradient Combinations”, *Iran. J. Mech. Eng. Technol.*, **16**(2), 5-25.
- Heydari, A. (2018), “Elastoplastic analysis of thick-walled vessels with isotropic strain hardening behavior using nonlinear compatibility relation”, *Proceedings of the 7th International Conference of Civil Engineering, Architecture and Urban Economy Development*, Shiraz, Iran.
- Heydari, A. (2019), “Elasto-plastic analysis of cylindrical vessel with arbitrary material gradation subjected to thermo-mechanical loading via DTM”, *Arab. J. Sci. Eng.*, **44**(10), 8875-8891. <https://doi.org/10.1007/s13369-019-03910-x>
- Heydari, A. and Jalali A.R. (2017), “A new scheme for buckling analysis of bidirectional functionally graded Euler beam having arbitrary thickness variation rested on Hetenyi elastic foundation”, *Modar. Mech. Eng.*, **17**(1), 47-55. <http://dorl.net/dor/20.1001.1.10275940.1396.17.1.17.7>
- Heydari, A. and Kazemi M.T. (2009), “Elasto-plastic analysis of thick walled tanks subjected to internal pressure”, *Int. J. Adv. Des. Manuf. Technol.*, **3**(1), 11-18. <https://sanad.iau.ir/Journal/admt/Article/873201>
- Kossakowski P.G. and Uzarska I. (2019), “Numerical modeling of an orthotropic RC slab band system using the Barcelona model”, *Adv. Comp. Des.*, **4**(3), 211-21, <https://doi.org/10.12989/acd.2019.4.3.211>
- Leu S.Y., Liao K.C. and Lin Y.C. (2014), “Plastic limit pressure of spherical vessels with combined hardening involving large deformation”, *Int. J. Pres. Ves. Pip.*, **114**, 16-22. <https://doi.org/10.1016/j.ijpvp.2013.11.007>
- Maleki M., Farrahi, G.H., Haghpanah Jahromi, B. and Hosseinian E. (2010), “Residual stress analysis of autofrettaged thick-walled spherical pressure vessel”, *Int. J. Pres. Ves. Pip.*, **87**(7), 396-401. <https://doi.org/10.1016/j.ijpvp.2010.04.002>
- Moghaddam, S. and R. Masoodi, A. (2019), “Elastoplastic nonlinear behavior of planar steel gabled frame”, *Adv. Comp. Des.*, **4**(4), 397-413. <https://doi.org/10.12989/acd.2019.4.4.397>
- Najibi, A. (2017), “Mechanical stress reduction in a pressurized 2D-FGM thick hollow cylinder with finite length”, *Int. J. Press. Vessels Pip.* **153**, 32-44. <https://doi.org/10.1016/j.ijpvp.2017.05.007>
- Oh S.T., Lee D.J., Yi S.T. and Jeong B.J. (2023), “Numerical analysis for dynamic characteristics of bridge considering next-generation high-speed train”, *Adv. Comp. Des.*, **8**(1), 1-12, <https://doi.org/10.12989/acd.2023.8.1.001>
- Polatov, A.M., Khaldjigitov, A.A. and Ikramov, A.M. (2020), “Algorithm of solving the problem of small elastoplastic deformation of fiber composites by FEM”, *Adv. Comp. Des.*, **5**(3), 305-321. <https://doi.org/10.12989/acd.2020.5.3.305>
- Sabzikar Boroujerdy, M. and Eslami, M.R. (2014), “Axisymmetric snap-through behavior of Piezo-FGM

- shallow clamped spherical shells under thermo-electro-mechanical loading”, *Int. J. Press. Vessels Pip.* **120-121**, 19-26. <https://doi.org/10.1016/j.ijpvp.2014.03.008>
- Sachdeva, C. and Padhee, S.S. (2018), “Asymptotically exact analytical formulations”, *Appl. Math. Model.* **54**, 782-802. <https://doi.org/10.1016/j.apm.2017.10.019>
- Saviz, M.R. (2017), “Electro-elasto-dynamic analysis of functionally graded cylindrical shell with piezoelectric rings using differential quadrature method”, *Acta Mech.* **228**(5), 1645-1670. <https://doi.org/10.1007/s00707-016-1746-7>
- Sim L.C., Yeo W.H., Purbolaksono J., Saw L.H. and Tey J.Y. (2021), “Analytical solution of thermo-mechanical stresses of multi-layered hollow spherical pressure vessel”, *Int. J. Pres. Ves. Pip.*, **191**, 104355. <https://doi.org/10.1016/j.ijpvp.2021.104355>
- Ushio, Y., Saruwatari, T. and Nagano, Y. (2019), “Elastoplastic FEM analysis of earthquake response for the field-bolt joints of a tower-crane mast”, *Adv. Comp. Des.*, **4**(1), 53-72. <https://doi.org/10.12989/acd.2019.4.1.053>
- Vatul’yan, A.O. and Yurov, V.O. (2016), “Wave processes in a hollow cylinder in an inhomogeneous prestress field”, *J. Appl. Mech. Tech. Phys.*, **57**(4), 731-739. <https://doi.org/10.1134/S0021894416040180>
- Yıldırım A., Yarımabaç D., Arikan V., Eker M. and Celebi K. (2022), “Nonlinear thermal stress analysis of functionally graded spherical pressure vessels”, *Int. J. Pres. Ves. Pip.*, **200**, 104830. <https://doi.org/10.1016/j.ijpvp.2022.104830>
- Zaid M. and Sadique Md. R., (2020), “Numerical modelling of internal blast loading on a rock tunnel”, *Adv. Comp. Des.*, **5**(4), 417-443, <https://doi.org/10.12989/acd.2020.5.4.417>

TK

Appendix

```

SUBROUTINE USDFLD(FIELD,STATEV,PNEWDT,DIRECT,T,CELENT,
  1 TIME,DTIME,CMNAME,ORNAME,NFIELD,NSTATV,NOEL,NPT,LAYER,
  2 KSPT,KSTEP,KINC,NDI,NSHR,COORD,JMAC,JMATYP,MATLAYO,LACCFLA)
C
  INCLUDE 'ABA_PARAM.INC'
C
  CHARACTER*80 CMNAME,ORNAME
  CHARACTER*3  FLGRAY(15)
  DIMENSION FIELD(NFIELD),STATEV(NSTATV),DIRECT(3,3),
  1 T(3,3),TIME(2)
  DIMENSION ARRAY(15),JARRAY(15),JMAC(*),JMATYP(*),COORD(*)

  FIELD(1)=SQRT(COORD(1)**2+COORD(2)**2+COORD(3)**2)

  RETURN
  END

```